

## Tunable Enhancement of High Harmonic Emission from Laser Solid Interactions

B. Dromey,<sup>1</sup> S. G. Rykovanov,<sup>2,4</sup> D. Adams,<sup>1</sup> R. Hörlein,<sup>2,5</sup> Y. Nomura,<sup>2</sup> D. C. Carroll,<sup>3</sup> P. S. Foster,<sup>6</sup> S. Kar,<sup>1</sup> K. Markey,<sup>1</sup>  
P. McKenna,<sup>3</sup> D. Neely,<sup>6</sup> M. Geissler,<sup>1</sup> G. D. Tsakiris,<sup>2</sup> and M. Zepf<sup>1,\*</sup>

<sup>1</sup>*Department of Physics and Astronomy, Queens University Belfast, BT7 INN, United Kingdom*

<sup>2</sup>*MPQ Garching, Hans-Kopfermann-Strasse 1, D-85748 Garching, Germany*

<sup>3</sup>*SUPA, Department of Physics, University of Strathclyde, Glasgow, G4 ONG, United Kingdom*

<sup>4</sup>*Moscow Physics Engineering Institute, Kashirskoe Shosse 31, 115409 Moscow, Russia*

<sup>5</sup>*Sektion Physik der Ludwig-Maximilians-Universität München, Am Coulombwall 1, D-85748 Garching, Germany*

<sup>6</sup>*Central Laser Facility, STFC Rutherford Appleton Laboratory, Chilton, Didcot, OX11 0QX, United Kingdom*

(Received 15 January 2009; published 4 June 2009)

Coherent wake emission is a unique source of extreme ultraviolet radiation and has been recently shown to provide the basis for intense attosecond light. Here we present a novel scheme, supported by particle-in-cell simulations, demonstrating that enhancement and spectral control of the coherent wake emission signal can be achieved by modifying the interaction plasma density ramp. Significant tunable enhancement of harmonic emission is verified experimentally, with factors of  $>50$  in relative signal increase achieved in a narrow band of harmonics at the cutoff frequency.

DOI: 10.1103/PhysRevLett.102.225002

PACS numbers: 52.35.Mw, 42.65.Ky, 52.27.Ny

Harmonic conversion processes at steep plasma-vacuum interfaces promise rapid advances in the generation of intense attosecond pulses [1,2] and provide an excellent diagnostic for the detailed and complex interaction of an intense laser with a solid target [3–8]. This is of key importance for applications such as the fast ignitor scheme for fusion [9] or laser driven ion accelerators [10], which depend sensitively on the plasma scale length and temporal shape of the laser pulse, with remarkable variations in thermal x-ray and radiation yields observed experimentally [3,4].

From the perspective of a source of intense vacuum ultraviolet (VUV) and extreme ultraviolet (XUV) attosecond pulses, harmonics generated from the plasma-vacuum interface have extremely exciting properties: near diffraction-limited spatial beam quality [5] with attosecond pulse duration [1] combines with high (compared to other approaches [11,12]) conversion efficiency. Importantly, in contrast to harmonic generation from gaseous media, where the peak pulse energy is limited by depletion of the medium through ionization, pulses with arbitrarily large energy can be converted at a plasma-vacuum interface while preserving the exceptional coherence properties of the driving laser [1,5,13]. Consequently, this process is well suited to the latest generation of petawatt class femtosecond lasers and should allow the production of attosecond pulses with mJ pulse energies [2].

Note that high order harmonic generation (HOHG) from solid density targets can be generated via two physically distinct processes: coherent wake emission (CWE) [1,6–8] and relativistically oscillating (plasma) mirror (ROM)[2–5,13,14]. CWE harmonics, which are the focus of this Letter, originate within the plasma density ramp at densities  $N_m = m^2 N_c$  ( $m$ : integer,  $N_c$ : critical density for driving laser frequency  $\omega_0$ ) that can be resonantly excited

by the electrostatic density waves associated with the bunches of Brunel electrons injected into the target once per laser cycle and emit electromagnetic waves via linear mode conversion. Since density oscillations can only be supported up to the maximum plasma frequency  $\omega_{p\max}$ , CWE harmonics can only be generated up to a maximum cutoff order  $n_{\max} = \omega_{p\max}/\omega_0 = (N_{\max}/N_c)^{1/2}$  [6,15]. CWE is typically the dominant process at lower intensities below around  $10^{19} \text{ W cm}^{-2} \mu\text{m}^2$  and provides an efficient means of generating harmonic radiation at wavelengths  $>20 \text{ nm}$ . Note that CWE is not a pure surface-only effect, but instead is intrinsically linked to evolving plasma conditions in the plasma density ramp.

ROM harmonics, on the other hand, are generated by the frequency upshift of radiation reflected from the critical density surface, which oscillates at relativistic velocities and in phase with the driving laser electric field [2,13,14]. Efficient ROM emission, characterized by power law efficiency scaling [3,5] occurs only for relativistic laser interactions ( $> 10^{18} \text{ W cm}^{-2} \mu\text{m}^2$ ) and extends to few Å wavelengths with high efficiency [3,4] in the relativistic limit [2,14].

While spectral modifications and enhancement are widely achieved by phase matching [11,12] the harmonic generation process in an extended gaseous medium similar approaches cannot be easily transferred to surface effects such as CWE and ROM. However, for CWE the cutoff frequency can be controlled by choosing materials of suitable density (e.g., for 800 nm laser polystyrene results in  $n_{\max} \sim 13$  and BK7 glass in  $n_{\max} \sim 19$ ). Additionally, it has been shown, both experimentally and theoretically, that CWE is very sensitive to preplasma levels and, therefore, the plasma scale length,  $L_s$  [16,17]. In particular, Tarasevitch *et al* [16] show using 1D PIC simulations optimally efficient CWE harmonic generation is achieved

for a short, but not infinitely steep, plasma gradient— $L_s > 0.1\lambda_{\text{Laser}}$ . Such optimal generation is demonstrated for all orders and monotonically decreasing efficiency of the harmonic spectrum is maintained. If the scale length is reduced below this optimum the monotonic harmonic efficiency decays rapidly.

However, the question still remains as to how the *shape* of the density profile effects generation. This is best investigated numerically using sufficiently short pulses to avoid the dynamic modification of the density ramp during the laser pulse [5,17], in effect allowing “snapshots” to be taken of what the CWE spectrum looks like for a fixed plasma density profile.

For a 3 cycle laser pulse incident at  $45^\circ$  with  $a_0 = 0.3$  interacting with a linear density ramp rising from 0 to  $200N_c$  (solid density) over 200 nm, the expected spectrum, from 1D PIC code PICWIG [18], is shown in Fig. 1(a). Containing harmonic orders due unambiguously to the coherent wake emission mechanism (since the interaction intensity is subrelativistic, i.e.,  $a_0 < 1$ ) the spectrum displays a characteristic slow decay, with all orders present, extending up the plasma frequency [corresponding to har-

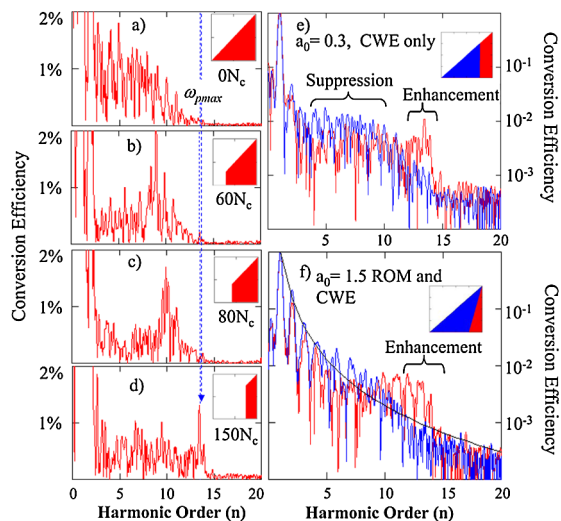


FIG. 1 (color online). Enhancement of CWE in 1D PIC simulations (mobile ions) via density profile modification for a 3 cycle  $1\ \mu\text{m}$  Gaussian laser pulse interacting with a target with linear plasma density ramp from 0 to solid density ( $200N_c$ ). Density profiles are steplike from 0 to an initial density ( $N_1$ ) followed by a linear ramp of  $(200 - N_1/N_c)$  nm up to the maximum density of  $200N_c$  (insets). Spectra obtained for  $N_1 = 0N_c, 60N_c, 80N_c,$  and  $150N_c$  and  $a_0 = 0.3$  are shown in (a)–(d). Part (e) shows a direct comparison of the spectra and density profiles shown in (a) (blue or dark gray trace and ramp) and (d) (red or gray trace and ramp). Part (f) is for  $a_0 = 1.5$  interacting with a linear density ramp rising from  $0N_c$  to  $200N_c$  over 200 nm (blue or dark gray trace in main and ramp in inset) and 50 nm (red or gray trace in main and ramp in inset). The apparent noisy nature of the CWE spectra presented is due to spectral splitting of harmonic orders resulting from the intensity dependent phase properties of CWE [8] which are dramatic for conditions of rapidly varying intensity, such as those in few cycle pulses.

monic cutoff order  $n_{\text{max}} \sim (N_{\text{max}}/N_c)^{1/2} = (200)^{1/2} \sim 14$ th harmonic]. However, modifying the linear density ramp to a combination of a steplike profile at a density  $N_1$  and a ramp of identical gradient from  $N_1$  to  $N_{\text{max}}$  has a dramatic effect on the observed spectrum [Figs. 1(b) and 1(d)]. For low values of  $N_1$ , shown in Figs. 1(b) and 1(c), the most notable effect is the suppression of midrange orders up to  $(N_1/N_c)^{1/2}$ . Together with the underlying decay to higher orders, this allows a tunable source of higher harmonic orders, i.e., only orders  $>7$ th emitted for step at  $60N_c$ ,  $>8$ th for step at  $80N_c$ . When the steplike profile is moved to near solid density [ $N_1 = 150N_c$ , Fig. 1(d)] the harmonics emitted are tuned to a narrow band around the maximum plasma frequency  $\omega_{p\text{max}}$  and a substantial enhancement of signal ( $>10$  times) is observed. This is the first demonstration of a departure from monotonically decreasing harmonic spectra described for generation from solid targets.

Physically, this spectral modification and subsequent enhancement can be interpreted as direct coupling of the laser energy (via Brunel electrons) to higher frequency resonant oscillations in the density profile, due primarily to the localization of the emission region for the  $m$ th harmonic to the part of the density ramp with a density of approximately  $N_m = m^2N_c$  [1,6–8]. Low order harmonic emission is suppressed due to the extremely steep density gradients in the vicinity of  $N_m$ , where the plasma oscillations are no longer efficiently excited. This weaker coupling to lower orders not only suppresses the low order harmonics, but also allows stronger excitation of the higher density plasma due to reduced energy loss of the electron bunch in the low density plasma. Note that the relative intensity of CWE harmonics carries information about the shape of the density profile in the ramp from  $N_c$  to  $N_{\text{max}}$  which is not obtainable by other methods.

The hybrid profiles (step + linear rise) studied in Fig. 1 are in fact simply an idealized case of the density profile in a ponderomotively steepened plasma with a laser pulse duration of tens of cycles. Figure 2 shows a 1D PIC simulation of the evolution of a plasma with an initial linear density ramp of 200 nm length from vacuum to solid density for a 40 fs pulse with  $a_0 = 7$ . The density profile steepens rapidly over the duration of the interaction with a particularly steep ramp forming for the densities corresponding to the midrange harmonics (compare  $\Delta x_1$  to  $\Delta x_2$  in Fig. 2), while the density profile for the highest harmonics remains largely unaffected. Clearly midrange orders will therefore be suppressed and the highest orders near the cutoff should be enhanced during the most intense part of the laser pulse. From this it is clear that the simulations performed in Fig. 1 for few cycle pulses essentially provide snapshots of the CWE spectrum expected from a plasma density that is evolving under the action of a longer, tens of cycle laser pulse.

The anticipated enhancement of harmonic orders near the plasma frequency was investigated using the Astra

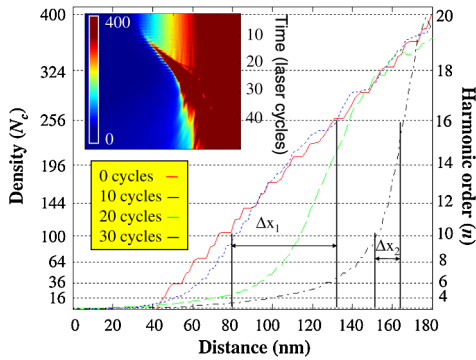


FIG. 2 (color online). Density profiles from 1D PIC simulation (mobile ions) showing the ponderomotive steepening of a 200 nm linear ramp from 0 to  $\sim 400N_c$  for a 45 fs pulse with  $a_0 = 7$ , with the peak of the pulse arriving at  $\sim 40$  cycles (inset Fig. 2). The horizontal dashed lines show the densities in the profile that correspond to the generation of a given harmonic order ( $n^2N_c$ ). Lineouts or density profiles are shown for 0 cycles (red, solid), 10 cycles (blue, dot), 20 cycles (green, dashed), and 30 cycles (black, dot-dashed).

titanium:sapphire laser at the Rutherford Appleton Laboratories, which delivered 800 mJ on target in 45 fs with a central wavelength of  $\lambda_{\text{laser}} \sim 800$  nm ( $p$ -polarized interaction). The pulse contrast was improved from a ratio  $\sim 10^8:1$  to  $\sim 10^{10}:1$  from peak to  $\sim 1$  ps prior to the main pulse by the use of a plasma mirror [19] which reduced the on-target energy to  $\sim 500$  mJ. The maximum intensity that could be delivered on target was estimated at  $2 \pm 0.5 \times 10^{19}$  W cm $^{-2}$  ( $a_0 \sim 3$ ). The target material was polished fused silica with a solid density of  $\sim 380N_c$ , implying that for these experimental conditions, the maximum harmonic order expected from the CWE process is  $n_{\text{max}} \sim 19$  which corresponds to the maximum plasma frequency. All orders above this are due unambiguously to ROM harmonic generation.

One of the key experimental challenges was to accurately diagnose or separate ROM and CWE for precise estimation of CWE harmonic enhancement on a given shot. For this, a specially designed XUV flatfield spectrometer allowed angular separation of the harmonic signal generated on a highly polished fused silica target (with sub 1 nm surface roughness) on a single shot basis (full description of setup given in [5]). ROM orders were observed to be beamed into  $\sim 19$  mrad  $1/e^2$  radius while CWE were observed to be beamed into  $>35$  mrad  $1/e^2$  radius [5].

Spectra for off and on specular axis emission generated for an intensity  $I_{\text{max}} = 1 \pm 0.5 \times 10^{19}$  W cm $^{-2}$  are shown in Figs. 3(a) and 3(b)-III. As can be seen the off-axis emission contains only harmonics up to the order corresponding to the plasma cutoff harmonic ( $n_{\text{max}} \sim 19$ ), and therefore CWE only, while the on-axis emission clearly contains orders extending beyond this to  $n = 26$ .

Experimental results for enhancement of CWE via density profile steepening are shown in Fig. 3(b). From the off-axis spectra (outside the diffraction-limited ROM cone

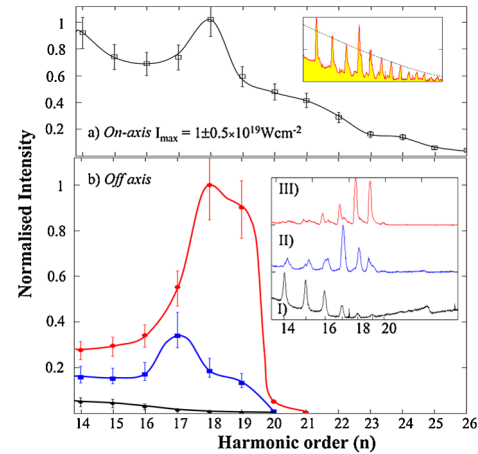


FIG. 3 (color online). Experimental results demonstrating the enhancement of CWE harmonics due to density profile steepening. Figures display a sum over the background subtracted signal in individual harmonic orders (bars show the spread in experimental data and uncertainty in the background subtraction) with lineouts of raw spectra obtained shown in the insets. Figure 3(a) contains the on-specular axis spectrum. Figure 3(b) contains the off-axis signals detected outside the diffraction-limited cone of the ROM harmonics (i.e., CWE orders only) for the following intensities (I)  $8 \pm 3 \times 10^{17}$  W cm $^{-2}$  (black, diamonds), (II)  $5 \pm 2 \times 10^{18}$  W cm $^{-2}$  (blue, boxes), (III)  $1 \pm 0.5 \times 10^{19}$  W cm $^{-2}$  (red, circles). The observed change in relative signal of harmonic orders is calculated from the ratio of  $n = 14$  and  $n = 19$  for (I) and (III), giving an enhancement factor of  $>50$ . The tunability of the enhancement is observed clearly in the transition from  $8 \pm 3 \times 10^{17}$  W cm to  $1 \pm 0.5 \times 10^{19}$  W cm $^{-2}$ .

angle and therefore containing only harmonics produced via CWE) shown in the inset of Fig. 3(b) it is clear that as intensity is increased there is a dramatic change in the shape of the observed CWE spectrum. For low intensities, the signal decays slowly towards  $\omega_{\text{max}}$  (black trace, filled diamonds) consistent with a ramp of sufficiently large gradient for all harmonic orders to be produced. However, as the intensity is increased the harmonic signal in higher orders is observed to be enhanced relative to lower orders, as can be seen in the blue (dark gray) and red (gray) traces. The observed factor relative enhancement between  $8 \pm 3 \times 10^{17}$  W cm $^{-2}$  to  $1 \pm 0.5 \times 10^{19}$  W cm $^{-2}$  for the 19th harmonic is  $>50$  (see Fig. 3 caption). For these experimental conditions the higher intensity gives a conversion efficiency of approximately  $5 \times 10^{-4}$  at  $\sim 42$  nm, corresponding to an energy of  $\sim 0.25$  mJ per harmonic peak per pulse.

The on-axis spectrum in Fig. 3(a) contains both CWE and ROM orders and has a very different overall spectral shape and content to that of the off-axis spectra. This spectrum can be compared directly to PIC simulations performed with  $a_0 = 1.5$  shown in Fig. 1(f), which also contain both ROM and CWE harmonics. For simulations with an initial ramp from  $0N_c$  to  $200N_c$  extending over 200 nm the spectrum is observed to decay slowly to higher orders [blue (dark gray) trace and ramp in inset], with a

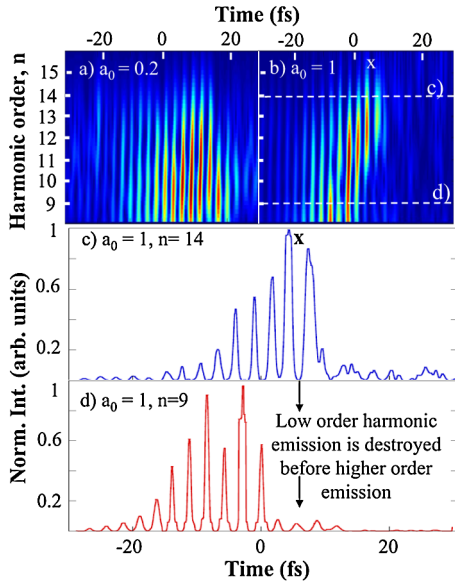


FIG. 4 (color online). Effect of increased intensity on the temporal evolution of solid target harmonic emission harmonic spectra. Time-frequency analysis of 1D PIC simulations (mobile ions) for a 40 fs Gaussian laser pulse incident at  $45^\circ$  on a  $200N_c$  maximum density plasma with a density ramp of 200 nm for two intensities, (a)  $a_0 = 0.2$  and (b)  $a_0 = 1$ . Clear departure from monotonically decaying spectra is demonstrated in (b). Lineouts of the temporal evolution of the 14th and 9th harmonics for  $a_0 = 1$  [white dashed lines in (b)] are shown in (c) and (d), respectively.

characteristic ROM power law scaling [2–4]. For simulations with a profile depth of 50 nm from  $0N_c$  to  $200N_c$  [red (gray) trace and ramp in inset] there is strong evidence of enhancement in the harmonic signal at the plasma frequency, identified as a clear departure from the power law scaling. Although this simulation [Fig. 1(f)] is performed for a 3 cycle pulse, and for lower target density, the fact that it is remarkably similar to the spectrum shown in Fig. 3(a), i.e., that of an enhanced CWE peak at  $\omega_{p \max}$  rising over the ROM background, is clear illustration that CWE enhancement via density profile steepening is robust.

Time-frequency analysis of PIC simulations performed using longer duration pulses (Fig. 4) show clearly that the principles derived from the fixed gradient PIC simulations of Fig. 1 are applicable under conditions where there is substantial profile steepening, permitting the observed enhancement.

In Fig. 4(a) a 45 fs pulse with low intensity ( $a_0 = 0.2$ ), and hence negligible profile steepening, demonstrates that the relative intensity of the harmonics barely vary from one optical cycle to the next and all harmonics peak in the cycles immediately after the peak of the laser pulse (time = 0 fs). For higher intensities [ $a_0 = 1$ , Fig. 4(b)], where profile steepening is significant, production efficiency of the midrange orders collapses before the peak of the pulse as expected from the evolution of the density

gradient [16] and only a narrow band of high harmonics near the cutoff is produced at the peak of the pulse. This demonstrates clear departure from monotonically decaying spectra expected for CWE [6,7]. Direct comparison of Fig. 4(b)  $a_0 = 1$ , intensity  $I \sim 1.38 \times 10^{18} \text{ W cm}^{-2} \mu\text{m}^{-2} \approx 2 \times 10^{18} \text{ W cm}^{-2}$  at 800 nm, and Fig. 3(b)-II with  $I = 5 \pm 2 \times 10^{18} \text{ W cm}^{-2}$  show excellent agreement between simulation and experiment for the enhancement of harmonics near the CWE cutoff.

In conclusion, we have demonstrated the first narrow-band enhancement of harmonics generated during intense laser solid target interaction. Importantly this enhancement has been shown to provide the basis for, not only a novel, tunable source of coherent XUV radiation, but also a powerful ultrafast plasma diagnostic, i.e., spectral enhancement at  $\omega_{p \max}$  indicates the onset of very steep plasma density gradient interactions. In summary this work improves the outlook for the accurate metrology of advanced plasma sources for ultrafast XUV pulses and ion beams.

We would like to acknowledge the support of the Astra Laser and Target Prep staff at RAL. M.Z acknowledges support from the Royal Society.

\*m.zepf@qub.ac.uk

- [1] Y. Nomura *et al.*, *Nature Phys.* **5**, 124 (2009).
- [2] G.D. Tsakiris, K. Eidmann, J. Meyer-ter-Vehn, and F. Krausz, *New J. Phys.* **8**, 19 (2006).
- [3] S.V. Bulanov, N.M. Naumova, and F. Pegoraro, *Phys. Plasmas* **1**, 745 (1994); B. Dromey *et al.*, *Nature Phys.* **2**, 456 (2006); T. Baeva, S. Gordienko, and A. Pukhov, *Phys. Rev. E* **74**, 046404 (2006).
- [4] B. Dromey *et al.*, *Phys. Rev. Lett.* **99**, 085001 (2007).
- [5] B. Dromey *et al.*, *Nature Phys.* **5**, 146 (2009).
- [6] F. Quere *et al.*, *Phys. Rev. Lett.* **96**, 125004 (2006).
- [7] C. Thaury *et al.*, *Nature Phys.* **3**, 424 (2007).
- [8] F. Quere *et al.*, *Phys. Rev. Lett.* **100**, 095004 (2008).
- [9] M. Tabak *et al.*, *Phys. Plasmas* **1** 1626 (1994).
- [10] E. Clark *et al.*, *Phys. Rev. Lett.* **84**, 670 (2000).
- [11] C.G. Durfee, A.R. Rundquist, S. Backus, C. Herne, M.M. Murnane, and H.C. Kapteyn, *Phys. Rev. Lett.* **83**, 2187 (1999); A. Paul *et al.*, *Nature (London)* **421**, 51 (2003).
- [12] M. Zepf, B. Dromey, M. Landreman, P.S. Foster, and S.M. Hooker, *Phys. Rev. Lett.* **99**, 143901 (2007).
- [13] L. Plaja *et al.*, *J. Opt. Soc. Am. B* **15**, 1904 (1998).
- [14] S. Gordienko, A. Pukhov, O. Shorokhov, and T. Baeva, *Phys. Rev. Lett.* **94**, 103903 (2005).
- [15] R.L. Carman, D.W. Forslund, and J.M. Kindel, *Phys. Rev. Lett.* **46**, 29 (1981).
- [16] A. Tarasevitch, K. Lobov, C. Wunsche, and D. von der Linde, *Phys. Rev. Lett.* **98**, 103902 (2007).
- [17] S.C. Wilks, W.M. Kruer, M. Takac, and A.B. Langdon, *Phys. Rev. Lett.* **69**, 1383 (1992).
- [18] S.G. Rykovanov *et al.*, *New J. Phys.* **10**, 025025 (2008).
- [19] B. Dromey *et al.*, *Rev. Sci. Instrum.* **75**, 645 (2004).